Influence of aging in the temperature range 250-350°C on the tribological performance of a WC-CoCr coating produced by HVOF

L. Rovatti[1], N.Lecis[1], D. Dellasega[2], V. Russo[2], E. Gariboldi[1]

[1]Politecnico di Milano, Dipartimento di Meccanica, Milan, Italy

[2]Politecnico di Milano, Dipartimento di Energia, Milan, Italy

Abstract

Coatings made of tungsten carbides in a metallic matrix are key materials for wear-resistant industrial components. However, the thermal stability could represent a critical parameter for the future development of these WC-based composites, in view of increasing their service temperature. In the present study the evolution after thermal exposure of a WC-CoCr coating deposited by HVOF in the temperature range 250-350°C up to 345 h was monitored. The analysis was carried out combining surface characterization (SEM, GDOES and Raman) with hardness and tribological behaviour. The results showed a detrimental effect of the oxidation on the wear behaviour of the WC-based material, already noticeable after short aging at the upper temperature. In fact, while in the untreated samples the worn products contributed to achieve a low and stable friction coefficient (COF), in the aged coatings a COF increase was observed. The worsening was due to the presence of porous and not-protective oxides grown during aging that overcome the lubricant oxidative effect occurred during sliding.

Keywords: WC-CoCr; HVOF; Aging; Wear; Oxidation

1. Introduction

High velocity oxygen fuel (HVOF) thermally sprayed coatings made of tungsten carbides (WC) are suitable for wear protection in various technology fields (e.g. in valves, aircraft landing gear, paper rolls, etc..) due to the unique combination of mechanical and chemical properties [1-2]. The WC carbide is characterized by noticeable wear performance, microhardness and thermal conductivity higher than other reinforcement phases [3-5]. On the other side, these WC-based coatings are known to undergo a fast oxidation that affects their tribological behaviour, contrary to other cermet materials [6]. Hence, even if the oxidation resistance can be improved by the chromium addition, the upper operating temperature in industrial applications is quite limited [7-8]. Recent studies showed that the wear properties of WC-CoCr coatings were significantly modified by air exposure already at 200°C [9]. Contradictory results of the oxidation effect on the tribological performance of WC-based coatings are reported in literature [7-11]. The reason can be related to the complexity of the oxide phases (CoO-WO_3, Cr_2O_3 and WO_3, etc..) that can grow on the WC-CoCr system at different temperatures in static or dynamic conditions. Recently researchers focused on the oxide formation on the WC-based coatings, after short term aging or during wear test at temperatures above 350°C [12].

The challenge of the present study was comparing the oxides grown during precise step of isothermal heat treatments at "intermediate" temperatures up to 350°C with the tribo-oxidation products formed during sliding test. The surface evolution was analysed through SEM, Raman, GDOES (Glow Discharge Optical Emission Spectroscopy) and microhardness measurements. Pin on disk test were carried out using a WC pin as counterpart, in order to reproduce the real working condition of an industrial component coupled with another WC-based material.

2. Experimental procedure

A commercial WC-10Co-4Cr powder with a size of 45 ± 15 μm was deposited on a substrate of ASTM A182 F51 stainless steel after grit-blasting with corundum. The size and the morphology of the powders employed can be observed in figure 1. The darker area contains mainly chromium and can be associated to Cr-rich carbides of type M_6C, typically detected in powders of the same composition (figure 1b) [10]. The coatings were deposited by HVOF process through the JP5000 torch with a powder feed rate of 100 g/min and using N_2 as powder carrier gas characterized by a pressure of 4 bar. The as-sprayed coatings were grinded to a nominal thickness of 250 μm, achieving a final roughness of $Ra < 0.1$ μm.

Three temperatures (250°C, 300°C and 350°C) and four aging steps (1h, 10 h, 100 h and 345 h) were selected for the heat treatments in air, as reported in table 1. In the table the codes corresponding to the different aging conditions can also be seen.

After aging, the coating surface was analysed by different characterization techniques: SEM, GDOES, microhardness, pin-on disk wear test and Raman spectroscopy. The GDOES signal was obtained through a sputtering process and the calibration of elemental concentration and of the erosion depth were carried out respectively with certified standards and by the optical profilometer Infinite Focus from Alicona (Graz, Austria). Morphology of the coatings have been assessed by a Zeiss Supra 40 field emission Scanning Electron Microscope (SEM, accelerating voltage 3-5 kV). The Vickers micro-hardness tests were performed on a Leica equipment, applying a load of 4.9 N

and repeating the measurement ten times for each condition. Wear tests were carried out using a CSM Instruments pin-on-disk tribometer, equipped with a WC ball (diameter of 6 mm) as a pin. This counterpart material was selected in order to verify the possible adhesive phenomena with the aged WC-based coating or during the sliding test. Under applied normal load of 5 N, the pin ran a circular path of 5 mm in diameter at linear speed of 0.1 m/s, for a distance of 500 m. After test, the corresponding tracks were observed by SEM in order to analyse the tribological behaviour of the different conditions. The wear rate was calculated according to the ASTM G99-05 standard test method, from the measurements obtained through the Alicona optical profilometer. Moreover, a thermocouple was welded on the pin in order to analyse the temperature evolution during the sliding test.

Stoichiometry and crystallography of the phases of the aged samples have been investigated by Raman Spectroscopy with a Renishaw InVia spectrometer in backscattering geometry using 514.5 nm excitation wavelength from an Ar ion laser.

3. Results

3.1 Microstructural characterization

SEM micrographs of the WC-CoCr coating cross-section in the as received state and after aging 345 h at 350 °C, are reported in figure 2a and b. Both coatings have a dense structure with a porosity lower than 1 % and made of tungsten carbide blocky shape particles characterized by an average size of 0.5 μm. No significant changes in the bulk microstructure were detected at these aging temperatures (compare figures 2c and d), but, in the top part of the coating exposed to the most severe conditions the presence of a not homogeneous porous oxidized layer was observed.

In particular, the interface between the oxide and the coating resulted to be irregular with different penetration depths of oxidation (see figures 2b and 3a).

The analysed porous structure of the oxide and the related EDS spectrum are reported in figure 3b and 3c.

3.2 Surface characterization: microhardness, GDOES, Raman analysis and wear results

Surface (SEM, GDOES, Raman spectroscopy) and mechanical analysis (hardness and the pin-on-disk wear test) were performed on the top surface in order to evaluate the effects of thermal exposure on the outer layer of the coatings.

Table 2 summarizes the microhardness values of the WC-CoCr coatings for the different aging conditions. After the thermal exposure, it was not possible to underline a relevant change in the microhardness that is localized in the range of 900-1000 HV with a standard deviation of 100-200 HV. The measured values correspond to those reported in literature for HVOF coatings of the same composition here evaluated [7-13].

Considering a slight influence of the heat treatments on microhardness, only aging conditions for temperatures higher than 250°C were more deeply analysed, expecting a more significant oxidation effect in this case. The GDOES profiles related to the oxygen and to the carbon concentrations are represented respectively in figure 4a and 4b.

A rise in the oxygen content in the first microns was detected in the long-term treated coatings. Correspondingly, a carbon depletion was measured at the top surface of the same samples. The results confirm that an oxidized layer was grown on the HVOF coatings during the long aging treatments. Oxidation degree is related both to aging temperature and time. But it is possible to see that temperatures higher than 350°C induce a faster oxidation and carbon depletion dynamics respect to 300°C.

The surfaces after aging treatments were analysed by Raman spectroscopy for the characterization of the oxide chemistry. Raman spectra for different exposure conditions are reported in figure 5a, specifying the main peaks of individuated oxides in the figure capture. In agreement with the GDOES results, no Raman signal was identified in the as received surface. The exposure to air at 300 °C for 100 h did not promote the formation of an oxide layer that can be detected by Raman. In fact no oxide peaks are present in the corresponding Raman spectrum and only a slight increase in oxygen content can be appreciated by GDOES analysis. Aging treatments for longer times (345 h) or higher temperatures (350 °C) promoted the oxidation of the HVOF coatings, as revealed by the Raman spectra in figure 5a, which all exhibit similar features. Peaks at about 183, 272, 698 and 810 cm^{-1} can be assigned to the monocline phase of WO_3 tungsten trioxide [14], which exhibits a good crystallinity with few stoichiometric defects. In addition, two broad weak bands at about 885 and 950 cm^{-1} may be appreciated. These two bands have been assigned to the mixed cobalt tungstate $CoWO_4$ and hydrated WO_3 ($WO_3 \cdot xH_2O$), respectively [12].

The coatings were analysed also by SEM, monitoring the evolution of the surface. No peculiar morphologies were observed in the as received coating, where just the grinding lines of the finishing process were detected (see figure 6a). At aging time and temperature higher than those of sample A12 (100h at 300°C), the coating became locally porous and some nanometric features appear on the surface (see figure 6b). As exposure time proceeds further, the surface was covered by extensive bulbous oxides, as it is visible in figures 6 c-d-e-f. Again it is possible to appreciate the faster and inhomogeneous oxidation related to temperatures above 350°C or to aging times higher than 100h, as it was already observed in the upper side of the cross section of the A7 condition (see figure 2b). In fact, the coating in Fig. 6c (300°C, 345 h) exhibits a morphology very similar to that of Fig. 6e (350°C, 100 h). The high magnification micrograph of figure 6d shows the nano-size structure of the porous oxidized area, likely referable to the WO_3 phase, in agreement with the Raman results.

The "sponge-like" structure of the WO_3 phase, compared to the more compact one of the complex MWO_4 oxides, was already detected by other authors [15]. This morphology can be due to the growth mechanism of the WO_3 oxide on the tungsten carbide particles with the possible release of CO and CO_2 gas [16]. These results are in agreement with the carbon depletion, measured by the GDOES analysis, in the outer layer of the heat treated coating (see figure 4b).

The wear resistance of the coatings was analysed by the sliding test after the different heat treatments. In figure 7 selected optical micrographs of the worn surface after the pin-on-disk test can be seen. Comparing the different conditions, it is possible to notice an increasing width of the wear tracks in correspondence of higher temperatures and longer aging conditions. It is also evident a peculiar colour, due to the oxidation, that characterizes the coatings after the different isothermal steps. In literature it is reported that slight changes in the ratio between oxygen and tungsten in the

WO_x phase can induce a modification in the oxide colour [17]. However, on the basis of the Raman and GDOES and Raman results the specific colours can be attributed to different thicknesses of the WO_3 oxide that has grown during aging and to the presence of mixed cobalt tungstate.

The aging effect on the friction coefficient in function of distance is represented in Fig. 8a. It is possible to observe that the COF has not a clear increasing trend with the aging time and temperature. In particular, an irregular behaviour can be underlined for the short-term aging treatments at the two analysed temperatures. This aspect will be discussed later on considering the Raman analysis on the worn tracks. However, a significant increase of the friction coefficient was measured for the conditions exposed to the longest times. In fact, if the COF value in the steady state condition is 0.23 for the as received WC-CoCr material, it reaches immediately values above 0.4 for the coating aged 345 h at 350°C.

Moreover, the wear rate for the short term aged coatings is in the range 10^{-7} mm^3/Nm, while for those aged 345 h at the temperatures of 300 °C and 350 °C are respectively almost two and four times higher (see the block diagram of figure 8b).

In order to verify the possible occurrence of oxidation during the sliding test, micro-Raman analysis were carried out also inside the wear tracks (see Fig. 5b). Concerning the two samples with no evident oxide on the surface (as received and 300 °C, 100 h), two broad bands around 800 cm^{-1} and 950 cm^{-1} are now present in their Raman spectrum. The first band may be ascribed at the formation of amorphous WO_3, while the second one is related to the formation of tungstite, a hydrous tungsten oxide ($WO_3 \cdot$ xH2O) [14-18]. Moving to samples that were annealed at intermediate conditions (300 °C, 345 h and 350 °C 100h), where WO_3 was already present, Raman spectra after the sliding test show a reduction and an amorphization of the WO_3, with a modification of the peaks detected in the corresponding aged coatings towards large bands. In addition the presence of the intense band at about 950 cm^{-1} reveals still the growth of the hydrate layer at the surface. Finally, on the coating aged in the extreme conditions (350 °C, 345 h) Raman features of both crystalline WO_3 and tungstite are clearly identified in the spectrum, with additional peaks at about 885 and 950 cm^{-1} related to the cobalt tungstate and to the hydrate with a lower relative intensity peak compared to the other aging conditions.

SEM characterization of the worn surface was carried out to deeply analyse the mechanisms occurred during the sliding test. Figure 9a and b show the wear tracks of the starting state coating. Small cracks in the tungsten carbides and the presence of oxidized material at the edges of the track can be pointed out. EDS microanalysis on the oxide confirmed the presence of O, W and smaller amount of Cr and Co (see figure 9b). Moreover, from the thermocouple welded on the pin a temperature around 30°C was measured. These results confirmed the possibility to produce, during the test, a tungsten-rich hydrate phase and a W-rich oxide, as proved also by the Raman analysis.

The material aged for 100 h showed slightly different worn surfaces in comparison with the as received material. Localized material removal in the oxidized area can be inferred by the micrographs reported in figure 9c and d, in particular for the condition exposed to the highest temperature. When the exposure time exceeded 100 h (as in the A13 and A7 coatings), the composite material local delamination phenomena of the oxide grown during aging (see the micrographs of figures 9e, f). Furthermore, plowing in the more oxidized regions (as shown in

figure 9f) was observed more evidently in the coating aged for 345h at 350°C (A7). These morphological observations are in agreement with the Raman, GDOES results and with the higher wear rate measured in the A7 coating exposed to the most severe conditions (see figure 8b). In fact, the presence of the un-protective and porous oxides could have promoted the removal of material during the sliding test.

Combining the surface analysis with the tribological results, a correspondence of the COF evolution with the oxidation state of the coatings can be underlined. In particular, the formation of amorphous WO_3 and tungstite in the as received condition, demonstrated to be beneficial for the wear performances of the coating, leading to a low and stable COF. Contrarily, long aging (345 h) at 350 °C produced a porous layer of crystalline WO_3 oxide and Co-tungstate that are not protective and decreases the wear resistance. This result can be related to the different lubricant nature of the formed oxides. As A. Erdemir reported in [19], the mixed CoO-WO_3 oxide is characterized by lower lubricant properties than the WO_3 one. Finally, at the intermediate conditions, the friction coefficient remained low if the beneficial effects of the oxide grown during sliding overcame the negative ones of the pre-existing oxides. These two competitive phenomena could explain the irregular behaviour of the COF (see figure 7a) measured for these conditions.

4. Conclusion

This study aimed to investigate the influence of different aging steps in air on a HVOF WC-CoCr coating. On the basis of the microhardness results and microstructural analysis in the selected temperature range no significant changes in the "bulk" were identified. Nevertheless, a negative influence of oxidation on the wear resistance of these WC-based coatings was pointed out. In particular, an increase of the friction coefficient was measured after aging at temperature above 250°C. As clarified by the Raman and GDOES analysis, the tribological properties are influenced by a competitive effect of the oxides grown during the isothermal treatments or during the sliding test. In fact, if the amorphous tungsten trioxide and the tungstite stabilize the friction coefficient during the wear test, not-protective crystalline WO_3 and mixed Co-rich oxides, grown during aging in air, decrease the tribological performance of these WC-based coatings.

Acknowledgements

The authors wish to thank Flame Spray S.p.A. that deposited the coatings and Valland spa, in particular G.A. Mondora and L. Mondora for providing the bulk material. The research was partly supported by VALCODERA PROJECT (VAL CODERA: VALve COating DEsign for high seRvice temperAture funded by Lombardy Region within "Bando Ricerca Innovazione 2014").

Bibliography

[1] J.K.N. Murthy, K. Satya Prasad, K. Gopinath, B. Venkataraman, Characterisation of HVOF sprayed Cr_3C_2-50(Ni20Cr) coating and the influence of binder properties on solid particle erosion behaviour, Surf. & Coat. Technol. 204 (2010) 3975–3985.https://doi.org/10.1016/j.surfcoat.2010.04.069.

[2] U. Selvadurai, P. Hollingsworth, I. Baumann, B. Hussong, W. Tillmann, S. Rausch, D. Biermann, Influence of the handling parameters on residual stresses of HVOF-sprayed WC-12Co coatings, Surf. & Coat. Technol. 268 (2015) 30–35. https://doi.org/10.1016/j.surfcoat.2014.11.055.

[3] H. Wang, T. Webb, J.W. Bitler, Study of thermal expansion and thermal conductivity of cemented WC–Co composite, Int. Journal of Refractory Metals and Hard Materials 49 (2015) 170–177. https://doi.org/10.1016/j.ijrmhm.2014.06.009.

[4] P. Chivavibul, M. Watanabe, S. Kuroda, K. Shinoda, Effects of carbide size and Co content on the microstructure and mechanical properties of HVOF-sprayed WC–Co coatings, Surf. & Coat. Technol. 202 (2007) 509–521. https://doi.org/10.1016/j.surfcoat.2007.06.026

[5] R.J.K. Wood, Tribology of thermal sprayed WC–Co coatings, Int. Journal of Refractory Metals and Hard Mater. 28 (2010) 82–94. https://doi.org/10.1016/j.ijrmhm.2009.07.011.

[6] E. Gariboldi, L. Rovatti N. Lecis, L. Mondora, G.A. Mondora, Tribological and mechanical behaviour of Cr_3C_2–NiCr thermally sprayed, coatings after prolonged aging, Surf. & Coat. Technol. 305 (2016) 83–92. https://doi.org/10.1016/j.surfcoat.2016.07.087.

[7] M. Jafari, M.H. Enayati, M. Salehi, S.M. Nahvi, C.G. Park, Comparison between oxidation kinetics of HVOF sprayed WC–12Co and WC–10Co–4Cr coatings, Int. J. Refract. Metals and Hard Mater. 41 (2013) 78–84. https://doi.org/10.1016/j.ijrmhm.2013.02.006.

[8] J.K.N. Murthy, B. Venkataraman, Abrasive wear behaviour of WC–CoCr and Cr3C2–20(NiCr) deposited by HVOF and detonation spray processes, Surf. & Coat. Technol. 200 (2006) pp.2642-2652. https://doi.org/10.1016/j.surfcoat.2004.10.136.

[9] J.A.R. Wesmann, N. Espallargas, Effect of atmosphere, temperature and carbide size on the sliding friction of self-mated HVOF WC–CoCr contacts, Tribology International 101 (2016) 301–313. https://doi.org/10.1016/j.triboint.2016.04.032.

[10] O.D. Greenwood, S.C. Moulzolf, P.J. Blau, R.J. Lad, The influence of microstructure on tribological properties of WO thin films, Wear 232 (1999) 84–90. https://doi.org/10.1016/S0043-1648(99)00255-0.

[11] G. Bolelli, L.-M. Berger, T. Börner, H. Koivuluoto, L. Lusvarghi, C. Lyphout, N.Markocsan, V. Matikainen, P. Nylén, P. Sassatelli, R. Trache, P. Vuoristo, Tribology of HVOF- and HVAF-sprayed WC–10Co4Cr hardmetal coatings: A comparative assessment, Surf. & Coat. Technol. 265 (2015) 125–144. https://doi.org/10.1016/j.surfcoat.2015.01.048.

[12] G. Bolelli, L.-M. Berger, M. Bonetti, L. Lusvarghi, Comparative study of the dry sliding wear behavior of HVOF-sprayed WC–$(W,Cr)_2C$–Ni and WC–CoCr hardmetal coatings, Wear 309 (2014) 96–111. https://doi.org/10.1016/j.wear.2013.11.001.

[13] D. Kunying, W. Lijun, S. Zhen, L. Yankuan, Effect of Isothermal Heat Treatment on Mechanical Properties of WC-17Co Coatings, Rare Metal Mater. and Eng. 43(10) (2014) 2365-2369. https://doi.org/10.1016/S1875-5372(14)60171-5.

[14] A. Baserga, V. Russo, F. Di Fonzo, A. Bailini, D. Cattaneo, C.S. Casari, A. Li Bassi, C.E. Bottani, Nanostructured tungsten oxide with controlled properties: Synthesis and Raman characterization, Thin Solid Films 515 (2007) 6465–6469. https://doi.org/10.1016/j.tsf.2006.11.067

[15] M. Jafari, M.H. Enayati, M. Salehi, S.M. Nahvi, J.C. Han, C.G. Park, High temperature oxidation behavior of micro/nanostructured WC-Co coatings deposited from Ni-coated powders using high velocity oxygen fuel spraying, Surf. & Coat. Technol. 302 (2016) 426–437. https://doi.org/10.1016/j.surfcoat.2016.06.044.

[16] S.A. Humphry -Baker, W. E. Lee, Tungsten carbide is more oxidation resistant than tungsten when processed to full density, Scripta Materialia 116 (2016) 67–70. https://doi.org/10.1016/j.scriptamat.2016.01.007

[17] E. Lassner, W.D. Schubert (1999), Tungsten, Properties, Chemistry, Technology of the Element, Alloys, and Chemical Compounds, Kluwer Academic/Plenum Publishers, New York (ISBN 0-306-45053-4).

[18] M.F. Daniel, B. Desbat, J.C. Lassegues, Infrared and Raman Study of WO_3 Tungsten Trioxides and WO_3, xH_2O Tungsten Trioxide Hydrates, J.of Solid State Chem. 67, 235-247 (1987). https://doi.org/10.1016/0022-4596(87)90359-8.

[19] A. Erdemir, A crystal-chemical approach to lubrication by solid oxides, Tribology Letters 8 (2000) 97–102. https://doi.org/10.1023/A:1019183101329.

Figure 1. SEM micrographs of the powders used for the HVOF deposition at two different magnifications and taken by: secondary (a) and backscattered electrons (b).

Figure 2. Cross section of the coatings: A in the as received state (a,c) and A7 aged for 345h at 350°C (b,d).

Figure 3. Top part of the cross section of the coating aged for 345h at 350°C (a). Detail of the oxide at higher magnification and related EDS microanalysis (b and c)

Figure 4. GDOES profiles of the oxygen and carbon concentration at increasing distance from the external coating surface after different aging treatments (a,b).

Figure 5. Raman spectra of: (a) air-aged WC-based coatings in different conditions and (b) the material inside the wear track after the pin-on-disk tests. Principal peaks of individuated oxides are evidenced: monocline WO_3 (triangle), $CoWO_4$ (square) and hydrated WO_3 ($WO_3 \cdot xH_2O$) (circle).

Figure 6. SEM micrographs of the coating surface in the as received state (a) in comparison with different aging conditions: 300°C 100h (b), 345h at 300°C (c and d), 350°C 100h (e) and 345h at 350°C (f).

Figure 7. Worn tracks after pin-on-disk test of the coatings in selected aging conditions.

Figure 8. COF behaviour in function of the sliding distance during the pin-on-disk test for the analysed WC-Co-Cr coatings (a) and summary of the wear rate after the pin-on-disk sliding test (b).

Figure 9. SEM micrographs of the coatings in the as received condition: inside and at the edge of the track (a, b) and inside the tracks after the following aging treatments: 100 h at 300 °C (c), 100 h at 350 °C (d), 345 h at 300 °C (e) and 345 h at 350 °C (f).

Table 1: Scheme of the isothermal treatments with the corresponding codes

T (°C) \ t (h)	0	1	10	100	345
20	A				
250		A1	A2	A3	
300		A9	A11	A12	A13
350		A4	A5	A8	A7

Table 2: Microhardness results on the coating surface in the analysed conditions

T (°C)	**t (h)**	**Code**	**Microhardness (HV)**
-	-	A	1059 ±125
250	1	A1	1098 ± 156
250	10	A2	1072 ±101
250	100	A3	981 ±150
300	1	A9	1033 ±151
300	10	A11	918 ±168
300	100	A12	1114 ±237
300	345	A13	892 ±133
350	1	A4	966 ±106
350	10	A5	1066 ±141
350	100	A8	1029 ±206
350	345	A7	1047 ±142

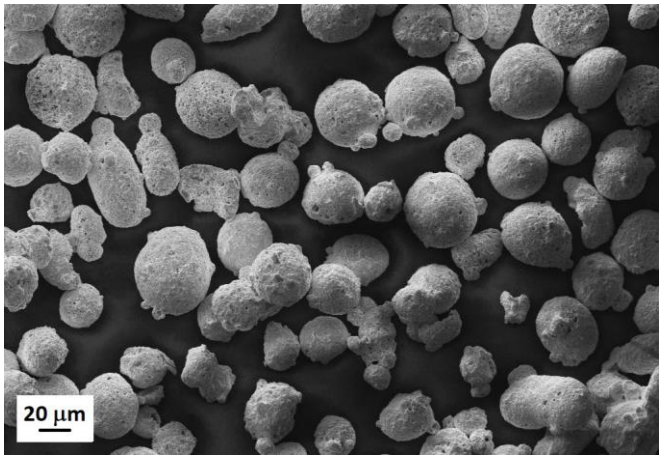

Fig: 1a

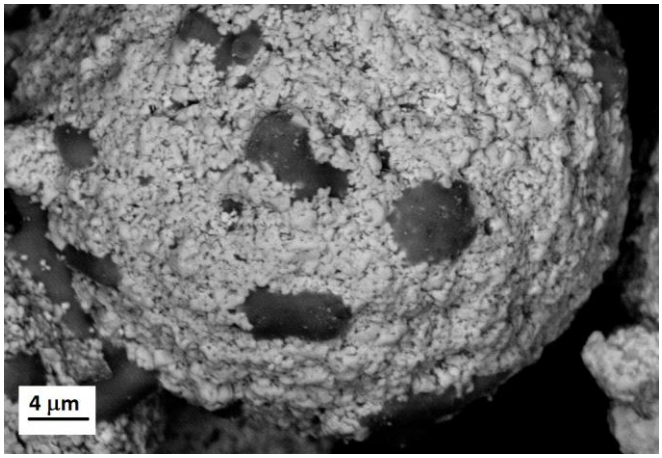

Fig: 1b

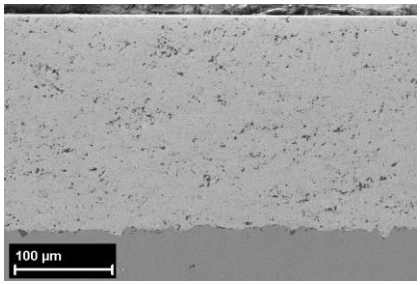

Fig: 2a

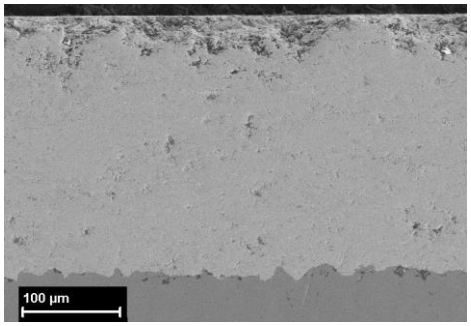

Fig: 2b

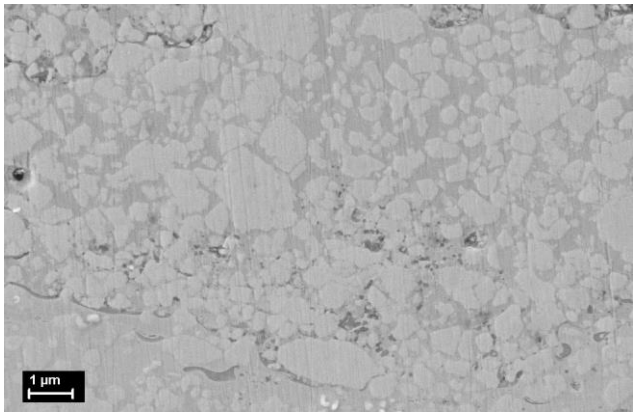

Fig: 2c

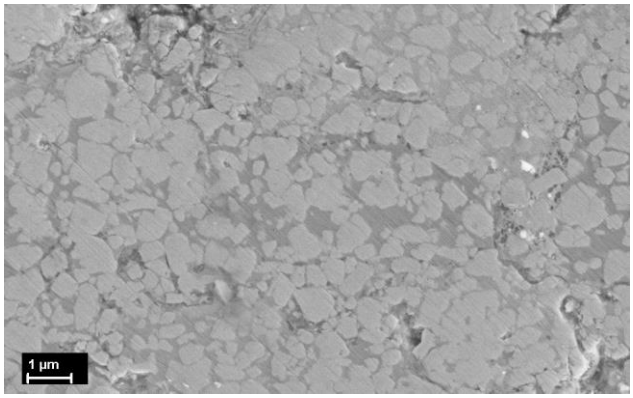

Fig: 2d

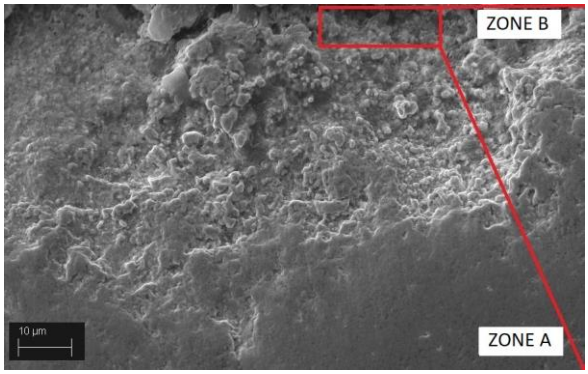

Fig: 3a

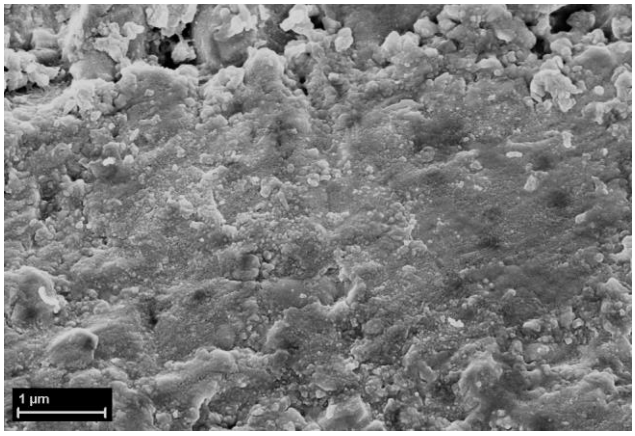

Fig: 3b

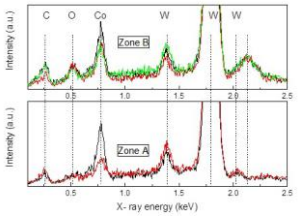

Fig: 3c

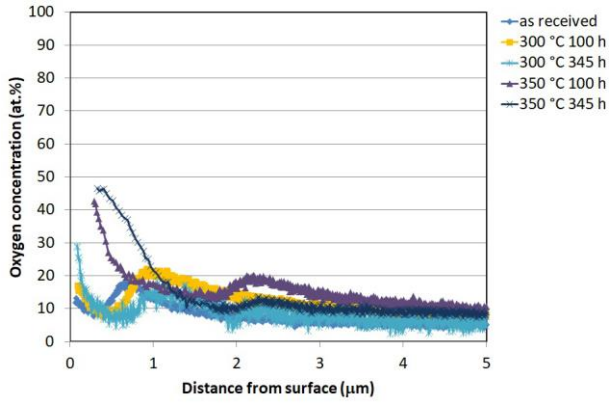

Fig: 4a

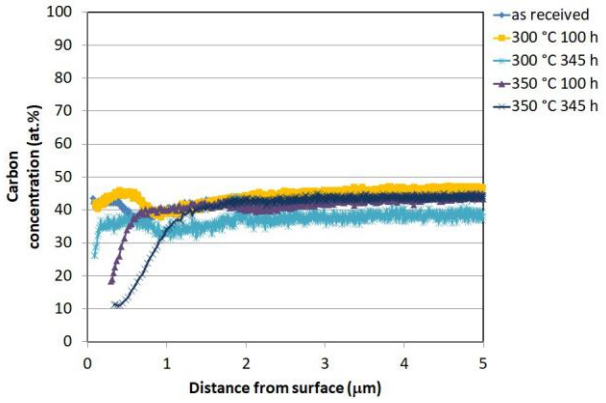

Fig: 4b

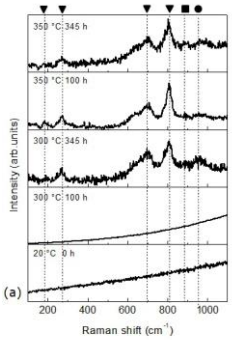

Fig: 5a

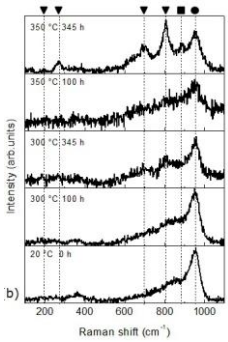

Fig: 5b

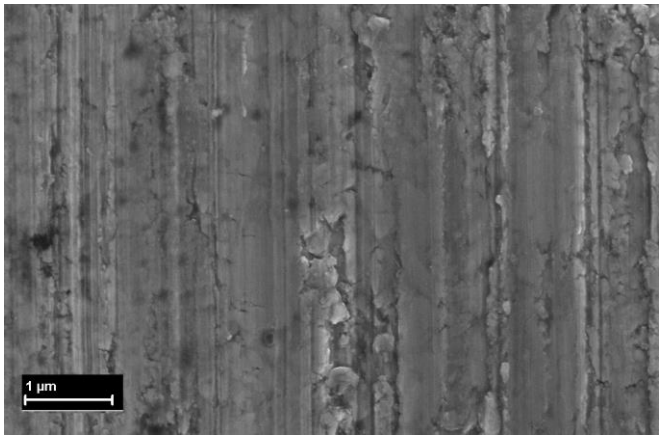

Fig: 6a

Fig: 6b

Fig: 6c

Fig: 6d

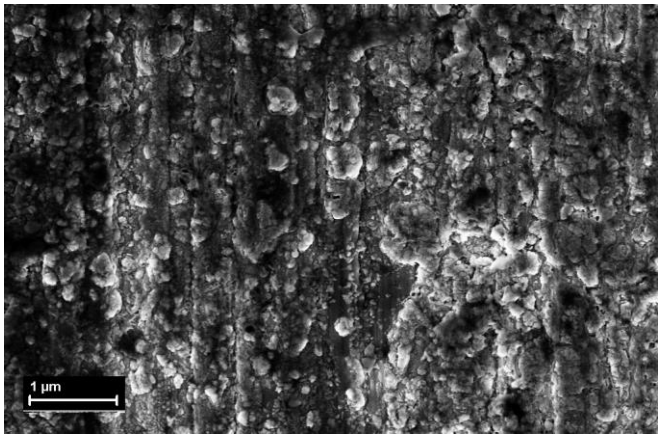

Fig: 6e

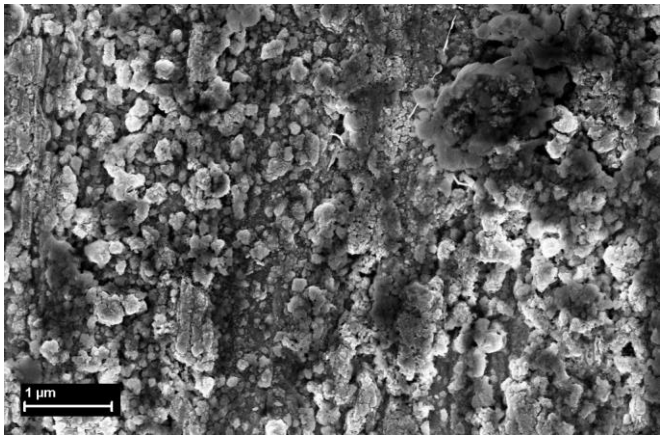

Fig: 6f

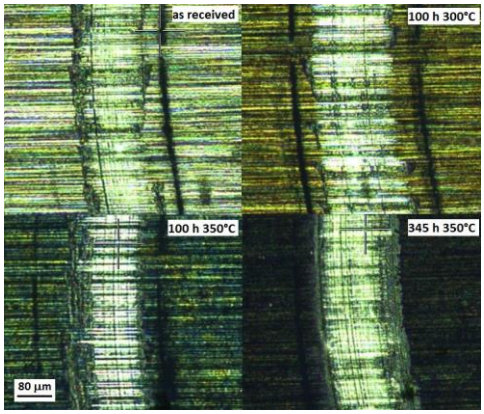

Fig: 7

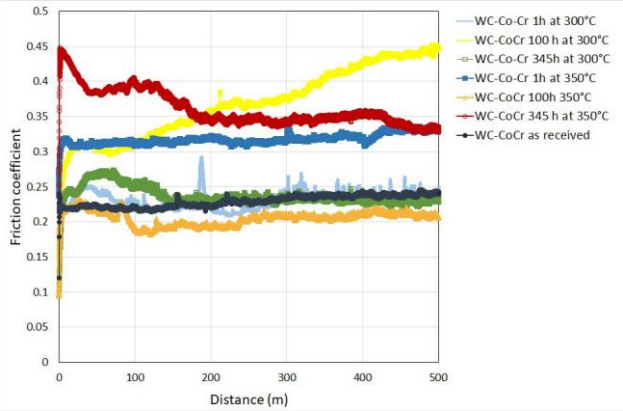

Fig: 8a

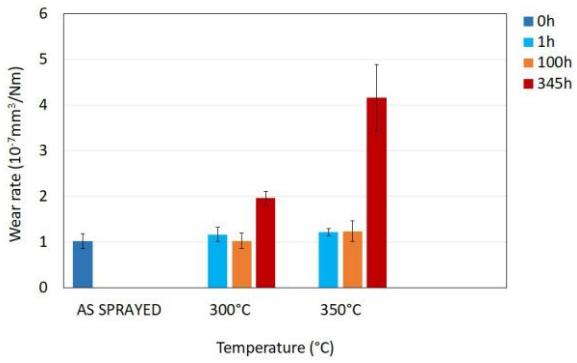

Fig: 8b

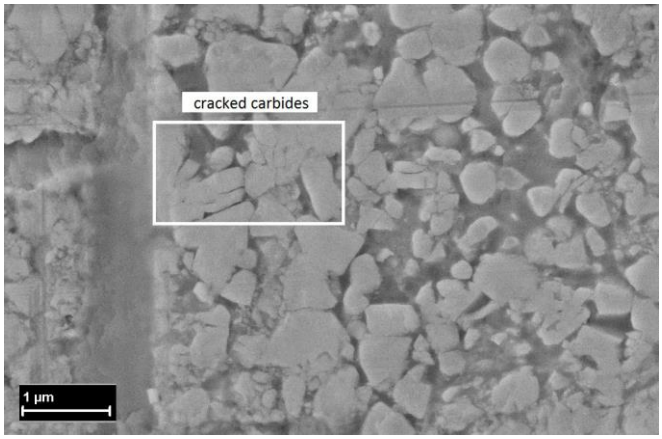

Fig: 9a

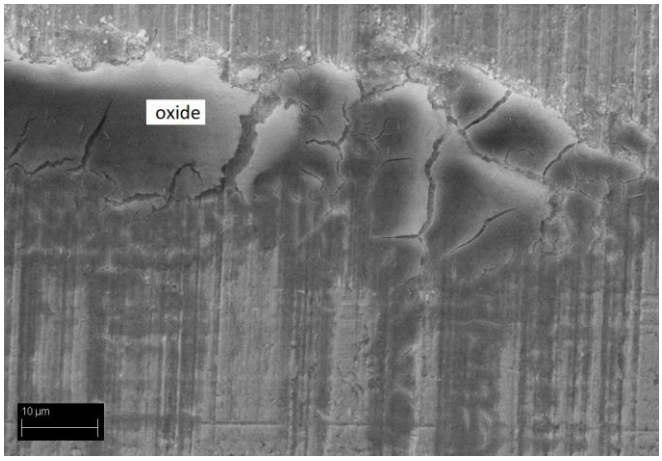

Fig: 9b

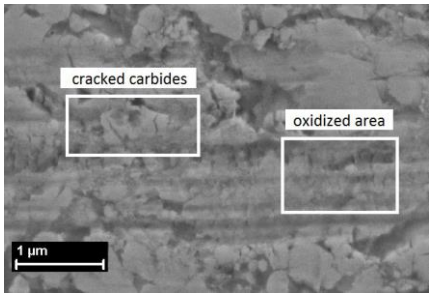

Fig: 9c

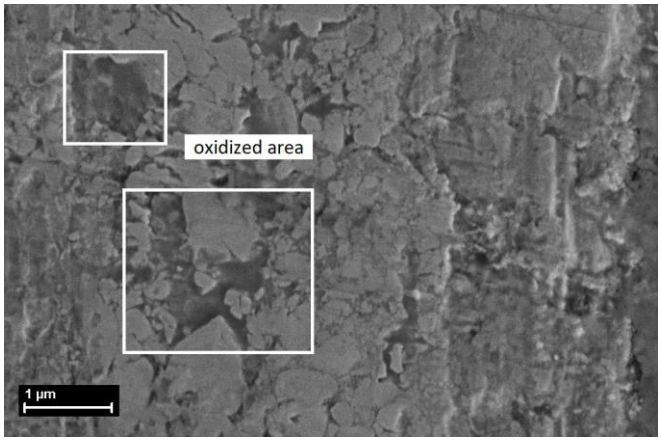

Fig: 9d

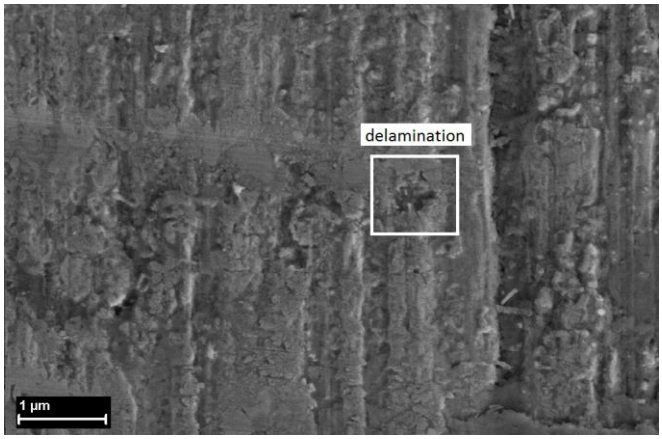

Fig: 9e

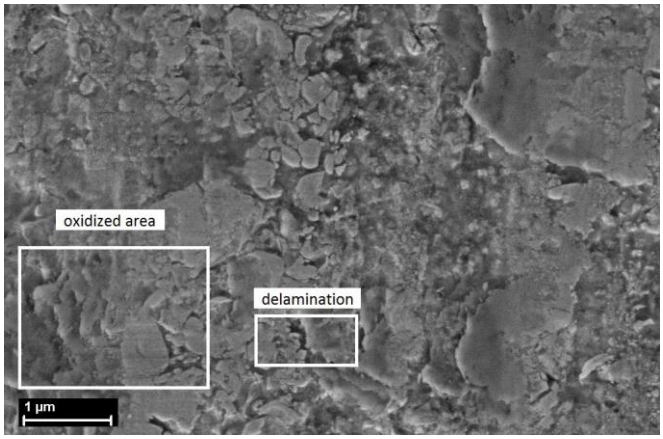

Fig: 9f

Graphical abstract

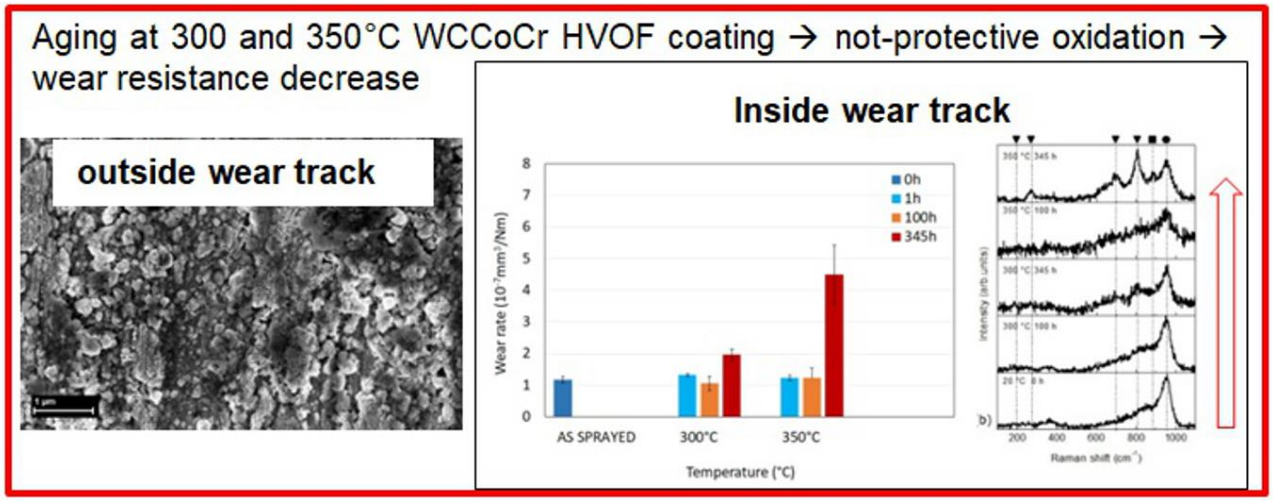

Highlights

- The effect of heat treatments in air on HVOF WCCoCr coatings is studied up to 350°C
- Surface evolution is characterized by hardness, pin on disk, GDOES, Raman and SEM
- The friction coefficient is below 0.25 in the as received coating
- Long aging produces not-protective oxides that increase wear rate and COF above 0.4